

# DISKS THAT ARE DOUBLE SPIRAL STAIRCASES

TOBIAS H. COLDING AND WILLIAM P. MINICOZZI II

There are many reasons for studying minimal surfaces. It was the birthplace of regularity theory. It lies on the intersection of nonlinear elliptic PDE, geometry, and low-dimensional topology and over the years the field has, through the efforts of many people, matured, yet some very fundamental questions remain. Moreover, many of the potentially spectacular applications have never been achieved. Surfaces with uniform area (or curvature) bounds have been well understood and the regularity theory is complete, yet essentially nothing was known without such bounds. We discuss here the theory of embedded minimal disks in  $\mathbf{R}^3$  without a priori bounds. As we will see the helicoid, which is a double spiral staircase, is the most important example of such a disk. In fact, we will see that every embedded minimal disk is either a graph of a function or is part of a double spiral staircase.

## What is a minimal surface and what are the examples?

Let  $\Sigma \subset \mathbf{R}^3$  be an orientable surface (possibly with boundary) with unit normal  $\mathbf{n}_\Sigma$ . Given  $\phi \in C_0^\infty(\Sigma)$ , define the one-parameter variation

$$\Sigma_{t,\phi} = \{x + t\phi(x)\mathbf{n}_\Sigma(x) | x \in \Sigma\}. \quad (1)$$

The so called first variation formula of area is the formula (integration is with respect to  $d\text{area}$ )

$$\frac{d}{dt} \Big|_{t=0} \text{Area}(\Sigma_{t,\phi}) = \int_\Sigma \phi H, \quad (2)$$

where  $H$  is the mean curvature of  $\Sigma$ .  $\Sigma$  is said to be a *minimal* surface (or just minimal) if

$$\frac{d}{dt} \Big|_{t=0} \text{Area}(\Sigma_{t,\phi}) = 0 \quad \text{for all } \phi \in C_0^\infty(\Sigma) \quad (3)$$

or, equivalently by (2), if the mean curvature  $H$  is zero. Thus  $\Sigma$  is minimal if and only if it is a critical point for the area functional. (The term “minimal” is misleading but time honored.) Moreover, a computation shows that if  $\Sigma$  is minimal, then

$$\frac{d^2}{dt^2} \Big|_{t=0} \text{Area}(\Sigma_{t,\phi}) = - \int_\Sigma \phi L_\Sigma \phi \quad \text{where } L_\Sigma \phi = \Delta_\Sigma \phi + |A|^2 \phi \quad (4)$$

is the second variational (or Jacobi) operator. Here  $\Delta_\Sigma$  is the Laplacian on  $\Sigma$  and  $A$  is the second fundamental form. So  $|A|^2 = \kappa_1^2 + \kappa_2^2$ , where  $\kappa_1, \kappa_2$  are the principal curvatures of  $\Sigma$  and  $H = \kappa_1 + \kappa_2$ .  $\Sigma$  is said to be stable if

$$\frac{d^2}{dt^2} \Big|_{t=0} \text{Area}(\Sigma_{t,\phi}) \geq 0 \quad \text{for all } \phi \in C_0^\infty(\Sigma). \quad (5)$$

One can show that a minimal graph is stable and, more generally, so is a multi-valued minimal graph (see below for the precise definition).

---

The authors were partially supported by NSF Grants DMS 0104453 and DMS 0104187.

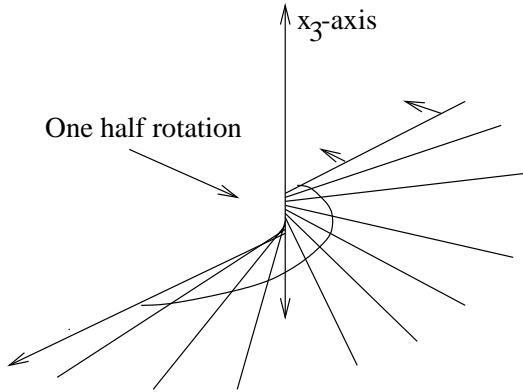


FIGURE 1. Multi-valued graphs. The helicoid is obtained by gluing together two  $\infty$ -valued graphs along a line.

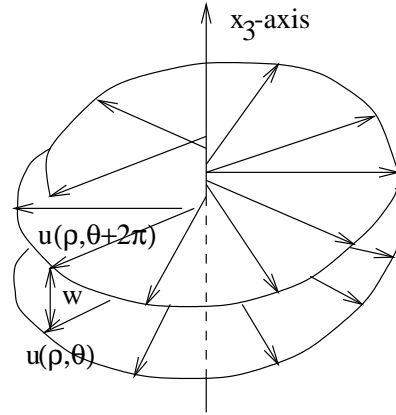


FIGURE 2. The separation  $w$  grows/decays at most sublinearly for a multi-valued minimal graph.

There are two local models for embedded minimal disks (by an *embedded disk* we mean a smooth injective map from the closed unit ball in  $\mathbf{R}^2$  into  $\mathbf{R}^3$ ). One model is the plane (or, more generally, a minimal graph) and the other is a helicoid intersected with a ball.

**Example 1:** (Minimal graphs). Graphs, i.e.,  $\{(x_1, x_2, u(x_1, x_2)) \mid (x_1, x_2) \in \Omega\}$ , of functions  $u : \Omega \rightarrow \mathbf{R}$  where  $\Omega \subset \mathbf{R}^2$  is a simply connected domain and  $u$  satisfies the minimal surface equation

$$\operatorname{div} \left( \frac{\nabla u}{\sqrt{1 + |\nabla u|^2}} \right) = 0. \quad (6)$$

A classical theorem of Bernstein says that entire (i.e., where  $\Omega = \mathbf{R}^2$ ) minimal graphs are planes.

The second model comes from the helicoid. The helicoid is a “double spiral staircase”, see fig. 0 (<http://www.a-castle-for-rent.com/castles/images/Chambord14.jpg>) that shows Leonardo da Vinci’s double spiral staircase in Chambord and fig. 00 (<http://images.amazon.com/images/P/0451627873.01.LZZZZZZZ.jpg>) that shows “the double helix” which was discovered by Crick and Watson as the structure of DNA. Also the internal ear, the cochlea, is a double spiral staircase; see fig. 000 or p. 343 of [K]. Other examples of double spiral staircases include parking ramps.

A *double spiral staircase* is two spiral staircases that spiral together. Thus two people could pass each other without meeting. For instance, one could go up on one staircase while the other goes down on the other staircase.

In the cochlea, the two canals winds around a conical bony axis and after about two and a half rotation they meet at the top and fuse. The canals are filled with fluids and sound waves travels up one canal, turn around, and come down the other. When the liquid is set into movement, it will then set the Basilar membrane and the hair cells into vibration. Different hair cells correspond to different frequencies.

**Example 2:** (Helicoid; see fig. 1). The minimal surface in  $\mathbf{R}^3$  parametrized by  $(s \cos t, s \sin t, t)$  where  $s, t \in \mathbf{R}$ .

To be able to give a precise meaning to the statement that the helicoid is a double spiral staircase we will need the notion of a multi-valued graph, each staircase will be a multi-valued graph, see fig. 1. Let  $D_r$  be the disk in the plane centered at the origin and of radius  $r$  and let  $\mathcal{P}$  be the universal cover of the punctured plane  $\mathbf{C} \setminus \{0\}$  with global polar coordinates  $(\rho, \theta)$  so  $\rho > 0$  and  $\theta \in \mathbf{R}$ . An  $N$ -valued graph on the annulus  $D_s \setminus D_r$  is a single valued graph of a function  $u$  over  $\{(\rho, \theta) \mid r < \rho \leq s, |\theta| \leq N\pi\}$ . The multi-valued graphs that we will consider will never close up; in fact they will all be embedded. Note that embedded corresponds to that the separation between the sheets (or the floors) never vanishes. Here the *separation* is the function (see fig. 2)

$$w(\rho, \theta) = u(\rho, \theta + 2\pi) - u(\rho, \theta). \quad (7)$$

If  $\Sigma$  is the helicoid, then  $\Sigma \setminus \{x_3 - \text{axis}\} = \Sigma_1 \cup \Sigma_2$ , where  $\Sigma_1, \Sigma_2$  are  $\infty$ -valued graphs on  $\mathbf{C} \setminus \{0\}$ .  $\Sigma_1$  is the graph of the function  $u_1(\rho, \theta) = \theta$  and  $\Sigma_2$  is the graph of the function  $u_2(\rho, \theta) = \theta + \pi$ . In either case the separation  $w = 2\pi$ . A *multi-valued minimal graph* is a multi-valued graph of a function  $u$  satisfying the minimal surface equation.

Note that for an embedded multi-valued graph, the sign of  $w$  determines whether the multi-valued graph spirals left-handed or right-handed. That is, as it spirals forward does it go clockwise or counterclockwise. For DNA, although both spirals occur, the right-handed spiral is far more frequent because of certain details of the chemical structure; see [CaDr].

One of the main theorems about embedded minimal disks is that such a disk can either be modeled by a minimal graph or by a piece of a rescaled helicoid depending on whether the curvature is small or not; see Theorem 1 below. Take a sequence  $\Sigma_i = a_i \Sigma$  of rescaled helicoids where  $a_i \rightarrow 0$ . (That is, rescale  $\mathbf{R}^3$  by  $a_i$ , so points that used to be distance  $d$  apart will in the rescaled  $\mathbf{R}^3$  be distance  $a_i d$  apart.) The curvatures of this sequence of rescaled helicoids are blowing up along the vertical axis. The sequence converges (away from the vertical axis) to a foliation by flat parallel planes. The singular set  $\mathcal{S}$  (the axis) then consists of removable singularities.

Throughout let  $x_1, x_2, x_3$  be the standard coordinates on  $\mathbf{R}^3$ . For  $y \in \Sigma \subset \mathbf{R}^3$  and  $s > 0$ , the extrinsic and intrinsic balls are  $B_s(y), \mathcal{B}_s(y)$ . That is,  $B_s(y) = \{x \in \mathbf{R}^3 \mid |x - y| < s\}$  and  $\mathcal{B}_s(y) = \{x \in \Sigma \mid \text{dist}_\Sigma(x, y) < s\}$ .  $K_\Sigma = \kappa_1 \kappa_2$  is the Gaussian curvature of  $\Sigma \subset \mathbf{R}^3$ , so when  $\Sigma$  is minimal (i.e.,  $\kappa_1 = -\kappa_2$ ), then  $|A|^2 = -2K_\Sigma$ .

See [CM1] (and the forthcoming book [CM3]) for background and basic properties of minimal surfaces and [CM2] for a more detailed survey and references.

### The limit foliation and the singular curve

In the next few sections, we will discuss the following; see fig. 3:

- A. If an embedded minimal disk  $\Sigma$  is not a graph (or equivalently if the curvature is large at some point), then it contains an  $N$ -valued minimal graph which initially is shown to exist on the scale of  $1/\max|A|$ .
- B. Such a potentially small  $N$ -valued graph sitting inside  $\Sigma$  can then be seen to extend as an  $N$ -valued graph inside  $\Sigma$  almost all the way to the boundary.
- C. Finally, one shows that it not only extends horizontally (i.e., tangent to the initial sheets) but also vertically (i.e., transversally to the sheets). That is, once there are  $N$  sheets there

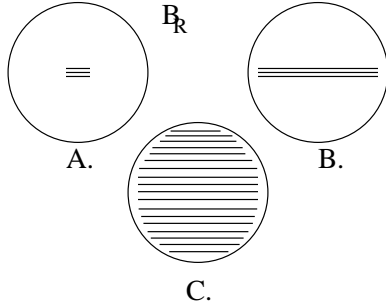


FIGURE 3. Proving Theorem 1. A. Finding a small  $N$ -valued graph in  $\Sigma$ . B. Extending it in  $\Sigma$  to a large  $N$ -valued graph. C. Extend the number of sheets.

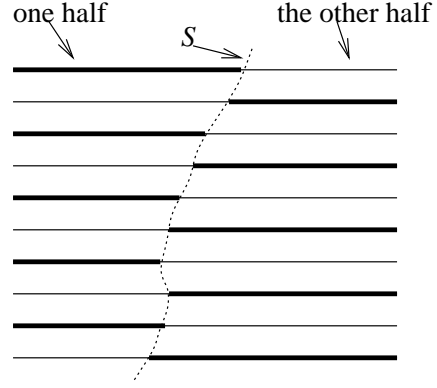


FIGURE 4. Theorem 1 - the singular set and the two multi-valued graphs.

are many more and, in fact, the disk  $\Sigma$  consists of two multi-valued graphs glued together along an axis.

A., B., and C. will be used to show:

**Theorem 1.** (See fig. 4). Let  $\Sigma_i \subset B_{R_i} = B_{R_i}(0) \subset \mathbf{R}^3$  be a sequence of embedded minimal disks with  $\partial\Sigma_i \subset \partial B_{R_i}$  where  $R_i \rightarrow \infty$ . If  $\sup_{B_1 \cap \Sigma_i} |A|^2 \rightarrow \infty$ , then there exists a subsequence,  $\Sigma_j$ , and a Lipschitz curve  $\mathcal{S} : \mathbf{R} \rightarrow \mathbf{R}^3$  such that after a rotation of  $\mathbf{R}^3$ :

1.  $x_3(\mathcal{S}(t)) = t$ . (That is,  $\mathcal{S}$  is a graph over the  $x_3$ -axis.)
2. Each  $\Sigma_j$  consists of exactly two multi-valued graphs away from  $\mathcal{S}$  (which spiral together).
3. For each  $\alpha > 0$ ,  $\Sigma_j \setminus \mathcal{S}$  converges in the  $C^\alpha$ -topology to the foliation,  $\mathcal{F} = \{x_3 = t\}_t$ , of  $\mathbf{R}^3$ .
4. For all  $r > 0$ ,  $t$ , then  $\sup_{B_r(\mathcal{S}(t)) \cap \Sigma_j} |A|^2 \rightarrow \infty$ .

In 2., 3. that  $\Sigma_j \setminus \mathcal{S}$  are multi-valued graphs and converges to  $\mathcal{F}$  means that for each compact subset  $K \subset \mathbf{R}^3 \setminus \mathcal{S}$  and  $j$  sufficiently large  $K \cap \Sigma_j$  consists of multi-valued graphs over (part of)  $\{x_3 = 0\}$  and  $K \cap \Sigma_j \rightarrow K \cap \mathcal{F}$ .

Here is a summary of the rest of the paper:

First we discuss some bounds for the separation of multi-valued minimal graphs. These bounds are used in both B. and C. above and we discuss what they are used for in C. In the following section we discuss the existence of multi-valued graphs, i.e., A. and B., and the important “one-sided curvature estimate”. Following that we explain how the one-sided curvature estimate is used to show that the singular set,  $\mathcal{S}$ , is a Lipschitz curve. The two last sections contain further discussion on the existence of multi-valued graphs and on the proof of the one-sided curvature estimate.

### Multi-valued minimal graphs - Towards removability of singularities

An important ingredient in the proof of Theorem 1 is that, just like the helicoid, general embedded minimal disks with large curvature at some interior point can be built out of  $N$ -valued graphs. By this, we mean that we will see that any embedded minimal disk can be divided into pieces each of which is an  $N$ -valued graph. Thus the disk itself should be

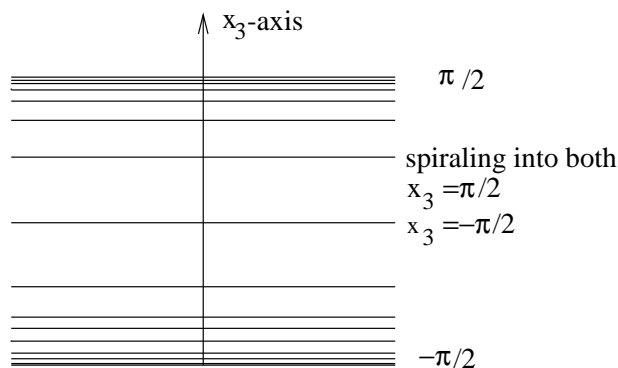


FIGURE 5. Properness; e.g., need to rule out that one of the multi-valued graphs can contain a graph like  $\arctan(\theta/\log \rho)$ , where  $(\rho, \theta)$  are polar coordinates.

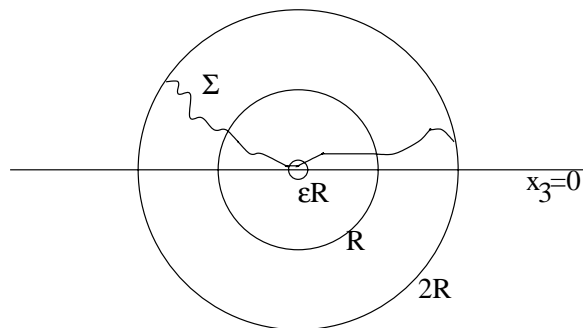


FIGURE 6. The one-sided curvature estimate for an embedded minimal disk  $\Sigma$  in a half-space: The components of  $B_R \cap \Sigma$  intersecting  $B_{\epsilon R}$  are graphs.

thought of as being obtained by stacking these pieces (graphs) on the top of each other. Even given such a decomposition, to prove Theorem 1, one still needs to analyze how the various  $N$ -valued pieces fit together. In particular, one needs to show that, just like the helicoid, an embedded minimal disk that is not a graph cannot be contained in a half-space; see Theorem 2 below and fig. 6. This is still not enough to imply Theorem 1. One also needs to show that part of any embedded minimal disk cannot accumulate in a half-space. This is what we call *properness* below; see fig. 5 and (10) that gives an example of an  $\infty$ -valued graph whose image lies in a slab in  $\mathbf{R}^3$ . The property we call properness is the assertion that no limit of embedded minimal disks can contain such a (nonproper) multi-valued graph.

In this section, we will discuss some analysis of embedded multi-valued graphs that is needed in the proof of Theorem 1. Two types of bounds for the growth/decay (as  $\rho \rightarrow \infty$ ) of the separation will be needed:

- a. The weaker sublinear bounds, i.e., for fixed  $\theta$  and  $\rho_0$ , the bounds

$$(\rho/\rho_0)^{-\alpha} |w(\rho_0, \theta)| \leq |w(\rho, \theta)| \leq (\rho/\rho_0)^\alpha |w(\rho_0, \theta)| \quad \text{as } \rho \rightarrow \infty, \quad (8)$$

where  $0 < \alpha < 1$ . These bounds holds for  $N$ -valued graphs (where  $N$  is some fixed large number). By letting  $N$  be large,  $\alpha$  can be chosen small.

- b. The stronger logarithmic bounds, i.e., for fixed  $\theta$  and  $\rho_0$ , the bounds

$$\frac{c_1}{\log(\rho/\rho_0)} |w(\rho_0, \theta)| \leq |w(\rho, \theta)| \leq c_2 \log(\rho/\rho_0) |w(\rho_0, \theta)| \quad \text{as } \rho \rightarrow \infty, \quad (9)$$

for constants  $c_1$  and  $c_2$ . These bounds will require a growing number of sheets (growing as  $\rho \rightarrow \infty$ ) and will be used only to show properness; cf. fig. 5.

(The sublinear bounds will be used in the proof of Theorem 2 below which in turn - through its corollary, Corollary 1 - is used to show that any multi-valued graph contained in an embedded minimal disk can be extended, inside the disk, to a multi-valued graph with a rapidly growing number of sheets and thus we get the better logarithmic bounds for the separation.)

By b. when the number of sheets grows sufficiently fast, the fastest possible decay for  $w(\rho, 0)/w(1, 0)$  is  $c_1/\log \rho$ . This lower bound for the decay of the separation is sharp. It is achieved for the  $\infty$ -valued graph of the harmonic function (graphs of multi-valued harmonic functions is a good model for multi-valued minimal graphs)

$$u(\rho, \theta) = \arctan \frac{\theta}{\log \rho}. \quad (10)$$

Note that the graph of  $u$  is embedded and lies in a slab in  $\mathbf{R}^3$ , i.e.,  $|u| \leq \pi/2$ , and hence in particular is not proper. On the top it spirals into the plane  $\{x_3 = \pi/2\}$  and on the bottom into  $\{x_3 = -\pi/2\}$ , yet it never reaches either of these planes; see fig. 5.

The next proposition rules out not only this as a possible limit of (one half of) embedded minimal disks, but, more generally, any  $\infty$ -valued minimal graph in a half-space.

**Proposition 1.** Multi-valued graphs contained in embedded minimal disks are proper - they do not accumulate in finite height.

### Existence of multi-valued graphs and the one-sided curvature estimate

We now come to the two key results about embedded minimal disks. The first says that if the curvature of such a disk  $\Sigma$  is large at some point  $x \in \Sigma$ , then near  $x$  a multi-valued graph forms (in  $\Sigma$ ) and this extends (in  $\Sigma$ ) almost all the way to the boundary. Moreover, the inner radius,  $r_x$ , of the annulus where the multi-valued graphs is defined is inversely proportional to  $|A|(x)$  and the initial separation between the sheets is bounded by a constant times the inner radius, i.e.,  $|w(r_x, \theta)| \leq C r_x$ .

As a consequence one easily gets that if  $|A|^2$  is blowing up near 0 for a sequence of embedded minimal disks  $\Sigma_i$ , then there is a sequence of 2-valued graphs  $\Sigma_{i,d} \subset \Sigma_i$ , where the 2-valued graphs start off defined on a smaller and smaller scale (the inner radius of the annulus where the multi-valued graphs is defined is inversely proportional to  $|A|$ ). Consequently, by the sublinear separation growth, such 2-valued graphs collapse. Namely, by the sublinear separation growth if  $\Sigma_{i,d}$  is a 2-valued graph over  $D_R \setminus D_{r_i}$ , then  $|w_i(\rho, \theta)| \leq (\rho/r_i)^\alpha |w_i(r_i, \theta)| \leq C \rho^\alpha r_i^{1-\alpha}$  for some  $\alpha < 1$  and some constant  $C$ . (In fact, by making  $N$  large,  $\alpha$  can be chosen small.) Letting  $r_i \rightarrow 0$  shows that  $|w_i(\rho, \theta)| \rightarrow 0$  for  $\rho, \theta$  fixed. Thus as  $i \rightarrow \infty$  the upper sheet collapses onto the lower and, hence, a subsequence converges to a smooth minimal graph through 0. (Here 0 is a removable singularity for the limit.) Moreover, if the sequence of such disks is as in Theorem 1, i.e., if  $R_i \rightarrow \infty$ , then the minimal graph in the limit is entire and hence, by Bernstein's theorem, is a plane.

The second key result is the following curvature estimate for embedded minimal disks in a half-space:

**Theorem 2.** (See fig. 6). There exists  $\epsilon > 0$ , such that if  $\Sigma \subset B_{2r_0} \cap \{x_3 > 0\} \subset \mathbf{R}^3$  is an embedded minimal disk with  $\partial\Sigma \subset \partial B_{2r_0}$ , then for all components  $\Sigma'$  of  $B_{r_0} \cap \Sigma$  which intersect  $B_{\epsilon r_0}$

$$\sup_{\Sigma'} |A_\Sigma|^2 \leq r_0^{-2}. \quad (11)$$

Using the minimal surface equation and that  $\Sigma'$  has points close to a plane, it is not hard to see that, for  $\epsilon > 0$  sufficiently small, (11) is equivalent to the statement that  $\Sigma'$  is a graph over the plane  $\{x_3 = 0\}$ .

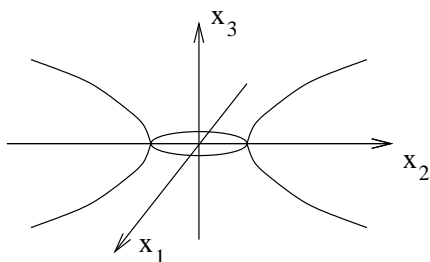


FIGURE 7. The catenoid given by revolving  $x_1 = \cosh x_3$  around the  $x_3$ -axis.

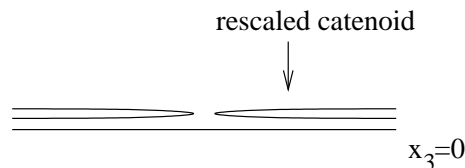


FIGURE 8. Rescaling the catenoid shows that simply connected is needed in the one-sided curvature estimate.

We will often refer to Theorem 2 as *the one-sided curvature estimate* (since  $\Sigma$  is assumed to lie on one side of a plane). Note that the assumption in Theorem 2 that  $\Sigma$  is simply connected (i.e., that  $\Sigma$  is a disk) is crucial as can be seen from the example of a rescaled catenoid. The catenoid, see fig. 7, is the minimal surface in  $\mathbf{R}^3$  given by  $(\cosh s \cos t, \cosh s \sin t, s)$  where  $s, t \in \mathbf{R}$ . Under rescalings this converges (with multiplicity two) to the flat plane; see fig. 8.

**Definition 1.** (Cones; see fig. 9). If  $\delta > 0$  and  $z \in \mathbf{R}^3$ , then we denote by  $\mathbf{C}_\delta(z)$  the (convex) cone with vertex  $z$ , cone angle  $(\pi/2 - \arctan \delta)$ , and axis parallel to the  $x_3$ -axis. That is, (see fig. 9)

$$\mathbf{C}_\delta(z) = \{x \in \mathbf{R}^3 \mid x_3^2 \geq \delta^2 (x_1^2 + x_2^2)\} + z. \quad (12)$$

In the proof of Theorem 1, the following (direct) consequence of Theorem 2 (with  $\Sigma_d$  playing the role of the plane  $\{x_3 = 0\}$ , see fig. 10) is needed (In words this corollary says that if an embedded minimal disk contains a 2-valued graph, then the disks consists of multi-valued graphs away from a cone with axis orthogonal to the 2-valued graph.):

**Corollary 1.** (See fig. 10). There exists  $\delta_0 > 0$  so: Suppose  $\Sigma \subset B_{2R}$ ,  $\partial\Sigma \subset \partial B_{2R}$  is an embedded minimal disk containing a 2-valued graph  $\Sigma_d \subset \mathbf{R}^3 \setminus \mathbf{C}_{\delta_0}(0)$  over  $D_R \setminus D_{r_0}$  with gradient  $\leq \delta_0$ . Then each component of  $B_{R/2} \cap \Sigma \setminus (\mathbf{C}_{\delta_0}(0) \cup B_{2r_0})$  is a multi-valued graph.

Fig. 10 illustrates how this corollary follows from Theorem 2. In this picture,  $B_s(y)$  is a ball away from 0 and  $\Sigma'$  is a component of  $B_s(y) \cap \Sigma$  disjoint from  $\Sigma_d$ . It follows easily from the maximum principle that  $\Sigma'$  is topologically a disk. Since  $\Sigma'$  is assumed to contain points near  $\Sigma_d$ , then we can let a component of  $B_s(y) \cap \Sigma_d$  play the role of the plane  $\{x_3 = 0\}$  in Theorem 2 and the corollary follows.

Using Theorems 1, 2, W. Meeks and H. Rosenberg proved that the plane and helicoid are the only complete properly embedded simply-connected minimal surfaces in  $\mathbf{R}^3$ .

### Regularity of the singular set and Theorem 1

By a very general compactness argument, it follows (after possibly going to a subsequence) that for a sequence of smooth surfaces there is a well defined notion of points where the second fundamental form of the sequence blows up. That is, let  $\Sigma_i \subset B_{R_i}$ ,  $\partial\Sigma_i \subset \partial B_{R_i}$ , and  $R_i \rightarrow \infty$  be a sequence of (smooth) compact surfaces. After passing to a subsequence,  $\Sigma_j$ , we may assume that for each  $x \in \mathbf{R}^3$  either (a) or (b) holds:

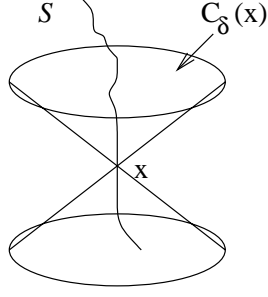


FIGURE 9. It follows from the one-sided curvature estimate that the singular set has the cone property and hence is a Lipschitz curve.

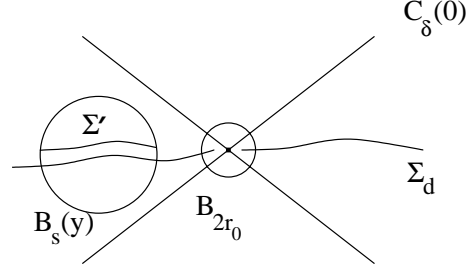


FIGURE 10. With  $\Sigma_d$  playing the role of  $\{x_3 = 0\}$ , by the one-sided estimate,  $\Sigma$  consists of multi-valued graphs away from a cone.

- (a)  $\sup_{B_r(x) \cap \Sigma_j} |A|^2 \rightarrow \infty$  for all  $r > 0$ ,  
 (b)  $\sup_j \sup_{B_r(x) \cap \Sigma_j} |A|^2 < \infty$  for some  $r > 0$ .

**Definition 2.** (Cone property). Fix  $\delta > 0$ . We will say that a subset  $\mathcal{S} \subset \mathbf{R}^3$  has the *cone property* (or the  $\delta$ -cone property) if  $\mathcal{S}$  is closed and nonempty and:

- (1) If  $z \in \mathcal{S}$ , then  $\mathcal{S} \subset \mathbf{C}_\delta(z)$ ; see Definition 1 for  $\mathbf{C}_\delta(z)$ .  
 (2) If  $t \in x_3(\mathcal{S})$  and  $\epsilon > 0$ , then  $\mathcal{S} \cap \{t - \epsilon < x_3 < t + \epsilon\} \neq \emptyset$  and  $\mathcal{S} \cap \{t - \epsilon < x_3 < t\} \neq \emptyset$ .

Note that (2) just says that each point in  $\mathcal{S}$  is the limit of points coming from above and below.

When  $\Sigma_i \subset B_{R_i} \subset \mathbf{R}^3$  is a sequence of embedded minimal disks with  $\partial \Sigma_i \subset \partial B_{R_i}$ ,  $R_i \rightarrow \infty$ ,  $\Sigma_j$  is the subsequence as above, and  $\mathcal{S}$  is the set of points where the curvatures of  $\Sigma_j$  blow up (i.e., where (a) above holds), then we will see below that  $\mathcal{S}$  has the cone property (after a rotation of  $\mathbf{R}^3$ ). Hence (by the next lemma),  $\mathcal{S}$  is a Lipschitz curve which is a graph over the  $x_3$ -axis. Note that when  $\Sigma_i$  is a sequence of rescaled helicoids, then  $\mathcal{S}$  is the  $x_3$ -axis.

**Lemma 1.** (See fig. 9). If  $\mathcal{S} \subset \mathbf{R}^3$  has the  $\delta$ -cone property, then  $\mathcal{S} \cap \{x_3 = t\}$  consists of exactly one point  $\mathcal{S}_t$  for all  $t \in \mathbf{R}$ , and  $t \rightarrow \mathcal{S}_t$  is a Lipschitz parameterization of  $\mathcal{S}$ .

Suppose next that  $\Sigma_i$  is as in Theorem 1 and  $\Sigma_j, \mathcal{S}$  are as above, then  $\mathcal{S}$  is closed by definition and nonempty by the assumption of Theorem 1. Centered at any  $x \in \mathcal{S}$  we can, by the existence of multi-valued graphs near points where the curvatures blow up, the sublinear separation growth, and Bernstein's theorem, find a sequence of 2-valued graphs  $\Sigma_{d,j} \subset \Sigma_j$  which converges to a plane through  $x$ ; see the discussion preceding Theorem 2. (This is after possibly passing to a subsequence of the  $\Sigma_j$ 's.) Thus (1) above holds by Corollary 1. Therefore to see that  $\mathcal{S}$  has the cone property all we need to see is that (2) holds. The proof of this relies on Proposition 1. Once the cone property of  $\mathcal{S}$  is shown, it follows from Lemma 1 that  $\mathcal{S}$  is a Lipschitz curve and by Corollary 1, away from  $\mathcal{S}$ , each  $\Sigma_j$  consists of multi-valued graphs. It is not hard to see that there are at least two such graphs and a barrier argument shows that there are not more.

### Blow up points and the existence of multi-valued graphs

To describe the existence of multi-valued graphs in embedded minimal disks, we will need the notion of a blow up point.

Let  $x \in \Sigma \subset B_{r_0}(x) \subset \mathbf{R}^3$  be a smooth (compact) surface embedded, or just immersed, with  $\partial\Sigma \subset \partial B_{r_0}(x)$ . Here  $B_{r_0}(x)$  is the extrinsic ball of radius  $r_0$  but could as well have been an intrinsic ball in which case the notion of a blow up point below would have to be appropriately changed. Suppose that  $|A|^2(x) \geq 4C^2 r_0^{-2}$  for some constant  $C > 0$ . We claim that there is  $y \in B_{r_0}(x) \cap \Sigma$  and  $s > 0$  such that  $B_s(y) \subset B_{r_0}(x)$  and

$$\sup_{B_s(y) \cap \Sigma} |A|^2 \leq 4C^2 s^{-2} = 4|A|^2(y). \quad (13)$$

That is, the curvature at  $y$  is large (this just mean that  $C$  should be thought of as a large constant) and is almost (up to the constant 4) the maximum on the ball  $B_s(y)$ . That there exists such a point  $y$  is easy to see; on  $B_{r_0}(x) \cap \Sigma$  set  $F(z) = (r_0 - r(z))^2 |A|^2(z)$  where  $r(z) = |z - x|$ . Then

$$F(x) \geq 4C^2, F \geq 0, \text{ and } F|_{\partial B_{r_0}(x) \cap \Sigma} = 0. \quad (14)$$

Let  $y$  be where the maximum of  $F$  is achieved and set  $s = C/|A|(y)$ . One easily checks that  $y, s$  have the required properties. Namely, clearly  $|A|^2(y) = C^2 s^{-2}$  and since  $y$  is where the maximum of  $F$  is achieved,

$$|A|^2(z) \leq \left( \frac{r_0 - r(y)}{r_0 - r(z)} \right)^2 |A|^2(y). \quad (15)$$

Since  $F(x) \geq 4C^2$  it follows from the choice of  $s$  that  $|r_0 - r(y)| \leq 2|r_0 - r(z)|$  for  $z \in B_s(y) \cap \Sigma$ . Hence,  $|A|^2(z) \leq 4|A|^2(y)$ . Together this gives (13).

The existence of multi-valued graphs is shown by combining a blow up result with an extension result. This blow up result says that if an embedded minimal disk in a ball has large curvature at a point, then it contains a small (in fact on the scale of  $1/\max|A|$ ) almost flat  $N$ -valued graph nearby; this is A. in fig. 3. The extension result allows us to extend the (small)  $N$ -valued graphs almost out to the boundary of the “big” ball  $B_R$ ; this is B. in fig. 3. In fact, the blow up result shows that if  $(y, s)$  is a blow up pair with point  $y$  and radius  $s > 0$  satisfying (13), then the corresponding  $N$ -valued function is defined on an annulus whose inner radius is  $s$  and so the initial separation is proportional to  $s$ . That is, for positive constants  $C_1, C_2$

$$C_1 s \leq |w(s, \theta)| \leq C_2 s. \quad (16)$$

Equation (16) will be used implicitly in the next section.

The extension result is significantly more subtle than the local existence. The key for being able to extend is a curvature estimate “between the sheets” for embedded minimal disks; see fig. 11. We think of an axis for such a disk  $\Sigma$  as a point or curve away from which the surface locally (in an extrinsic ball) has more than one component. With this weak notion of an axis, the estimate between the sheets is that if one component of  $\Sigma$  is sandwiched between two others that connect to an axis, then there is a fixed bound for (the norm of) the curvature of the one that is sandwiched. The example to keep in mind is a helicoid and the components are “consecutive sheets” away from the axis. Once the estimate between the sheets is established, then it is applied to the “middle” sheet(s) of an  $N$ -valued graph to show that even as we go far out to the “outer” boundary of the  $N$ -valued graph the curvature has a fixed bound. Using this a priori bound and additional arguments one gets

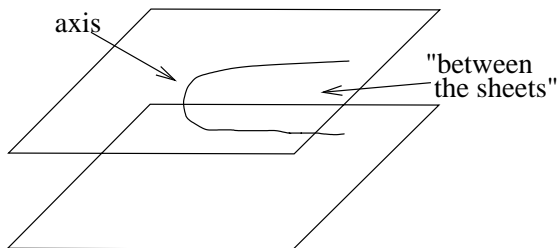


FIGURE 11. The curvature estimate “between the sheets.”

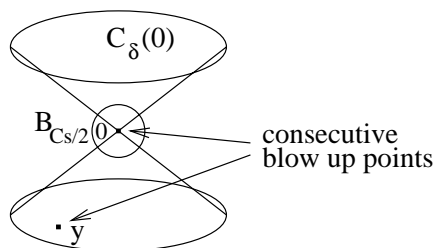


FIGURE 12. Two consecutive blow up points satisfying (18).

better bounds and eventually (with more work) argue that the sheets must remain almost flat and thus the  $N$ -valued graph will remain an  $N$ -valued graph.

### The proof of the one-sided curvature estimate

Using a blow up argument and the minimal surface equation, one can show curvature estimates for minimal surfaces which on all sufficiently small scales lie on one side of, but come close to, a plane. Such an assumption is a scale invariant version of Theorem 2. However, the assumption of Theorem 2 is not scale invariant and the theorem cannot be proven this way. The scale invariant condition is very similar to the classical Reifenberg property. (After all, a subset of  $\mathbf{R}^n$  has the Reifenberg property if it is close on all scales to a hyper-plane; see the appendix of [ChC].) As explained above (in particular Corollary 1), the significance of Theorem 2 is indeed that it only requires closeness on one scale. On the other hand, this is what makes it difficult to prove (the lack of scale invariance is closely related to the lack of a useful monotone quantity).

Let us give a very rough outline of the proof of the one-sided curvature estimate; i.e., Theorem 2. Suppose that  $\Sigma$  is an embedded minimal disk in the half-space  $\{x_3 > 0\}$ . The curvature estimate is proven by contradiction; so suppose that  $\Sigma$  has low points with large curvature. Starting at such a point, we decompose  $\Sigma$  into disjoint multi-valued graphs using the existence of nearby points with large curvature (the existence of such nearby points is highly nontrivial to establish. We will use that such a nearby point of large curvature can be found below any given multi-valued graph and thus we can choose the “next” blow up point to always be below the previous). The key point is then to show (see Proposition 2 below) that we can in fact find such a decomposition where the “next” multi-valued graph starts off a definite amount below where the previous multi-valued graph started off. In fact, what we show is that this definite amount is a fixed fraction of the distance between where the two graphs started off. Iterating this eventually forces  $\Sigma$  to have points where  $x_3 < 0$ . This is the desired contradiction.

To show this key proposition (Proposition 2), we use two decompositions and two kinds of blow up points. The first decomposition uses the more standard blow up points given as pairs  $(y, s)$  where  $y \in \Sigma$  and  $s > 0$  is such that

$$\sup_{B_{8s}(y)} |A|^2 \leq 4|A|^2(y) = 4C_1^2 s^{-2}. \quad (17)$$

The point about such a pair  $(y, s)$  is that  $\Sigma$  contains a multi-valued graph near  $y$  starting off on the scale  $s$ . (This is assuming that the curvature at  $y$  is sufficiently large, i.e.,  $C_1$  is a

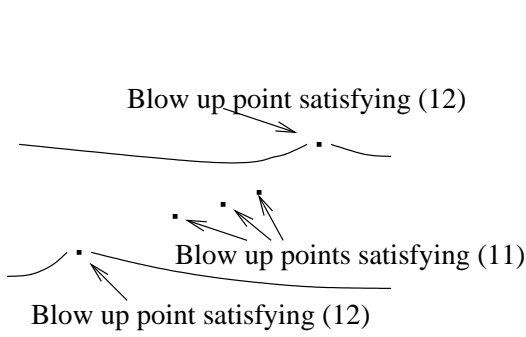


FIGURE 13. Between two consecutive blow up points satisfying (18) there are a bunch of blow up points satisfying (17).

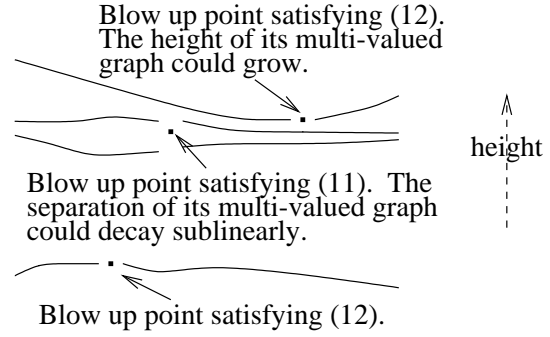


FIGURE 14. Measuring height. Blow up points and corresponding multi-valued graphs.

sufficiently large constant.) The second kind of blow up points are the ones where (except for a technical issue)  $\delta$  in the radius of the ball centered at  $y$  is replaced by some really large constant  $C$ , i.e.,

$$\sup_{B_{Cs}(y)} |A|^2 \leq 4|A|^2(y) = 4C_1^2 s^{-2}. \quad (18)$$

**Proposition 2.** (See fig. 12). There exists  $\delta > 0$  such that if point 0, radius  $s$  satisfies (18) and  $\Sigma_0 \subset \Sigma$  is the corresponding (to  $(0, s)$ ) 2-valued graph over  $D_R \setminus D_s$ , then we get point  $y$ , radius  $t$  satisfying (18) with  $y \in C_\delta(0) \cap \Sigma \setminus B_{Cs/2}$  and where  $y$  is below  $\Sigma_0$ .

The point for proving Proposition 2 is that we can find blow up points satisfying (18) so that the distance between them is proportional to the sum of the scales. Moreover, between consecutive blow up points satisfying (18), we can find a bunch of blow up points satisfying (17); see fig. 13. The advantage is now that if we look between blow up points satisfying (18), then the height of the multi-valued graph given by such a pair grows like a small power of the distance whereas the separation between the sheets in a multi-valued graph given by (17) decays (at the worst) like a small power of the distance; see fig. 14. Now, thanks to that the number of blow up points satisfying (17) (between two consecutive blow up points satisfying (18)) grows almost linearly, then, even though the height of the graph coming from the blow up point satisfying (18) could move up (and thus work against us), the sum of the separations of the graphs coming from the points satisfying (17) dominates the other term. Thus the next blow up point satisfying (18) (which lies below all the other graphs) is forced to be a definite amount lower than the previous blow up point satisfying (18). This gives the proposition.

Theorem 2 follows from the proposition. Suppose the theorem fails; starting at a point of large curvature and iterating the proposition will eventually give a point in the minimal surface with  $x_3 < 0$ , which is a contradiction.

We are grateful to Christian Berg, Chris Croke, Camillo De Lellis, Paul Schlapobersky, David Ussery, and David Woldbye for suggestions and comments and we are particularly grateful to Andrew Lorent for his very many very helpful comments.

## REFERENCES

- [ChC] J. Cheeger and T. H. Colding, On the Structure of Spaces with Ricci Curvature Bounded Below; I, *Jour. of Diff. Geometry* 46 (1997) 406-480.
- [CM1] T.H. Colding and W.P. Minicozzi II, Minimal surfaces, Courant Lecture Notes in Math., v. 4, 1999.
- [CM2] T.H. Colding and W.P. Minicozzi II, Embedded minimal disks, To appear in The Proceedings of the Clay Mathematics Institute Summer School on the Global Theory of Minimal Surfaces. MSRI.
- [CM3] T.H. Colding and W.P. Minicozzi II, Minimal surfaces in 3-manifolds, Graduate studies in Mathematics, AMS, in preparation.
- [CaDr] C.R. Calladine and H.R. Drew, Understanding DNA, Academic Press 1997.
- [K] W. Kahle, Color Atlas and textbook of human anatomy, vol. 3, Nervous system and sensory organs, Georg Thieme verlag, 3ed., 1986.

COURANT INSTITUTE OF MATHEMATICAL SCIENCES AND PRINCETON UNIVERSITY, 251 MERCER STREET,  
NEW YORK, NY 10012 AND FINE HALL, WASHINGTON RD., PRINCETON, NJ 08544-1000

DEPARTMENT OF MATHEMATICS, JOHNS HOPKINS UNIVERSITY, 3400 N. CHARLES ST., BALTIMORE,  
MD 21218

*E-mail address:* colding@cims.nyu.edu, minicozz@jhu.edu